JOURNAL OF VIROLOGY, Dec. 1991, p. 6654–6660
0022-538X/91/126654-07$02.00/0

Vol. 65, No. 12

Viral Persistence during the Developmental Phase of Coxsackievirus B1-Induced Murine Polymyositis

PATRICIA E. TAM,[1]* ANDREW M. SCHMIDT,[1] STEVEN R. YTTERBERG,[1,2] AND RONALD P. MESSNER[1]

Department of Medicine, University of Minnesota Medical School, Box 108, University of Minnesota Health Center, 420 Delaware Street S.E., Minneapolis, Minnesota 55455,[1] and Veterans Administration Medical Center, Minneapolis, Minnesota 55417[2]

Received 18 June 1991/Accepted 10 September 1991

Mice infected with coxsackievirus B1 (CVB1) develop a chronic hindquarter muscle weakness which resembles human polymyositis. In this study, we used in situ hybridization to screen for persistent viral RNA in hamstring and quadriceps muscles from mice that displayed various degrees of clinical weakness. At 28 to 31 days postinfection, when chronic myositis is well developed but infectious virus can no longer be recovered, persistent CVB1 RNA was found in hindquarter skeletal muscle of all 12 infected animals examined. Persistent CVB1 showed a multifocal distribution within muscle and was associated with three different histopathology patterns (HPPs). These three HPPs (HPP-1, HPP-2, and HPP-3) represent potentially different stages in the mechanism of persistence. They are based on the pattern of grains, the location of hybridization signal within the muscle, and the accompanying histopathology. In HPP-1, virus persisted in nonnecrotic muscle fibers and was not directly associated with foci of inflammatory cells. HPP-2 consisted of virus contained within necrotic myocytes that were surrounded by inflammatory cells. HPP-3 was rare and showed virus inside infiltrating mononuclear cells in a region where muscle tissue had been extensively destroyed. Persistent CVB1 occurred more frequently in severely diseased animals and in tissue sections displaying intense inflammation. Moreover, HPP-2 showed a stronger association with tissue inflammation and hindquarter weakness than did HPP-1. These data demonstrate that CVB1 persists in skeletal muscle for at least 28 to 31 days postinfection and support the concept that this persistence plays a role in the development of murine polymyositis.

There is increasing evidence that enteroviruses are involved in the pathogenesis of certain myopathies and that they persist in the afflicted tissue (1, 4, 8, 16, 17). Several studies have implicated enteroviruses as possible etiologic agents in human polymyositis (PM) and dermatomyositis. Among them, Travers et al. have shown that neutralizing titers of antibody to coxsackievirus are sometimes associated with disease development in PM patients (21), and infectious coxsackievirus has been recovered from stool samples of some patients with recent-onset PM (15). More recently, molecular approaches using cDNA probes derived from enterovirus genomes have identified viral RNA in muscle biopsy specimens from some patients with adult PM, adult dermatomyositis, and juvenile dermatomyositis (2, 12, 22). Positive biopsy specimens obtained from patients with a duration of symptoms of up to 4 years suggest that enterovirus persistence is a factor in the maintenance of these chronic inflammatory myopathies (22).

In one animal model of enterovirus-induced myopathy, infection of certain strains of neonatal mice with coxsackievirus B1 (CVB1) causes a chronic myositis which shows clinical and histologic similarities to human PM (11, 18, 23). Acute inflammation with myonecrosis is seen in tissue sections by day 2 postinfection. Strains of mice that do not develop chronic myositis show a resolution of acute inflammation by day 10 with subsequent regeneration of normal muscle tissue. In susceptible strains, acute inflammation is replaced by perivascular and perifascicular mononuclear cell infiltrates. Muscle regeneration occurs as the acute inflammation subsides, but it is not complete. Thereafter, myonecrosis and regeneration occur together. Clinically, these animals develop a proximal hindquarter muscle weakness which ranges from mild to extremely severe. In the latter case a flexion deformity may occur, rendering the limb completely useless. Also, an asymmetric distribution is often observed, with one leg being more affected than the other. Electromyogram abnormalities are consistent with inflammatory myopathy rather than neuropathy (18), and T cells are required for chronic disease expression, suggesting that autoimmunity plays a role in pathogenesis (24, 25).

During acute infection with CVB1, virus titers in hindquarter muscle peak at day 7 and remain positive for at most 2 weeks (18, 23). After this time, virus cannot be cultured from any tissue. Viral RNA has been detected in muscle at day 10 by using a probe derived from a cDNA clone of CVB3 (26). However, since chronic weakness perseveres for at least 10 weeks (18, 23), it is pertinent to screen for CVB1 at later times. In an effort to determine whether CVB1 persists and if persistence contributes to the development of chronic myositis, we have examined hindquarter skeletal muscle for the presence of viral RNA at 28 to 31 days postinfection by using in situ hybridization. Our results demonstrate that CVB1 RNA persists in three distinct locations within muscle and that the level of persistence correlates with the severity of clinical weakness and inflammation. This suggests that, in murine PM, CVB1 persistence contributes to the expression of chronic myositis.

MATERIALS AND METHODS

Virus. The myotropic Tucson strain of CVB1 (18) was propagated in Buffalo green monkey kidney (BGMK) cells according to previously described procedures (23, 24). Briefly, cell-free supernatants from disrupted monolayers of infected BGMK cells were pooled, titers were used to

* Corresponding author.

determine the number of PFU, and the supernatants were stored at −70°C.

Mice. Within 48 h after birth, specific-pathogen-free Swiss CD-1 mice (Charles River Laboratories, Inc., Wilmington, Mass.) were injected intraperitoneally with 200 to 2,000 PFU of CVB1. An average mortality of 30% resulted from the acute infection. No mortality was observed in the control population of animals injected with an equivalent amount of supernatant from uninfected BGMK cells. At 28 to 31 days postinfection, survivors were evaluated for the presence of clinical disease. Some asymmetry was observed, and so each leg was evaluated individually on a scale of 0 to 3 as follows: grade 0, no visible disease; grade 1, leg is slightly splayed but can still be used to walk and grip a wire screen; grade 2, leg drags visibly with little or no ability to grip; grade 3, leg is contracted toward the body and cannot be used to walk or grip. Serologic tests for *Mycoplasma pulmonis*, Sendai virus, and murine hepatitis virus were negative for each of four animals tested.

Tissue. Following evaluation of clinical weakness, mice were anesthetized with methoxyflurane and sacrificed by cervical dislocation. The hamstring and quadriceps muscles from each leg were removed, sliced longitudinally, and submerged in freshly prepared chilled 5% paraformaldehyde dissolved in 0.14 M phosphate-buffered saline (PBS). The muscle was fixed for 24 h, dehydrated by stepwise immersion in 50 and 70% ethanol for 24 h each, and stored in 80% ethanol at 4°C. Paraffin-embedded tissue was cut into 8-μm sections and covalently bound to gamma-aminopropyltriethoxy silane-treated glass slides as described by Tourtellotte et al. (19). Sections were stored at 4°C until processed for in situ hybridization. Hamstring and quadriceps muscles from the left and right hind limbs of 6 control and 12 infected animals were screened by in situ hybridization.

Hybridization probes. The plasmid pCB3-M1, which contains a complete cDNA clone of CVB3 inserted into p2732B, was provided by Reinhard Kandolf (Max Planck Institute for Biochemistry, Martinsried, Germany) (9). To prepare an enterovirus-specific probe, pCB3-M1 was cut with *Eco*RI to completely excise the insert. The resulting 2.7- and 4.8-kb fragments were purified by electroelution from agarose gels (14) and labeled with ^{35}S-dATP and ^{35}S-dCTP (1,200 Ci/mmol) (NEN, Boston, Mass.) by nick translation according to the manufacturer's protocol (Promega Corp., Madison, Wis.). The vector p2732B was labeled for use as a negative control to evaluate the specificity of hybridization. A cDNA clone of mouse α-actin (pAM 91) was used as a positive control probe (10). The probes were composed of fragments of 100 to 500 bp in length as determined on alkaline agarose gels, and they had specific activities ranging from 1.7×10^8 to 4.2×10^8 dpm/μg.

In situ hybridization. In situ hybridization was performed according to the method of Haase et al. with minor modifications (6). Briefly, the sections were deparaffinized, washed twice in 95% ethanol, and dried. They were then made permeable by treating for 30 min at room temperature in 0.2 M HCl, 15 min at room temperature in 0.1 M triethanolamine (pH 7.4), and 15 min at 37°C in proteinase K (40 μg/ml in 20 mM Tris-HCl–2 mM $CaCl_2$, pH 7.4). The slides were dipped in water, immersed in 0.1 M triethanolamine (pH 8.0), and acetylated by adding acetic anhydride to 0.25% with stirring for 10 min at room temperature. The slides were then washed twice with water and dehydrated through graded ethanol solutions of 70, 80, and 100% (5 min each). The hybridization mixture contained the DNA probe (200 ng/ml), 50% deionized formamide, 2.5% dextran sulfate, 0.1 mM aurintricarboxylic acid, 100 μg of sonicated salmon sperm DNA per ml, 10 μg of poly(A) per ml, 600 mM NaCl, 20 mM HEPES (*N*-2-hydroxyethylpiperazine-*N*′-2-ethanesulfonic acid), 1 mM EDTA, 0.02% polyvinylpyrrolidone, 0.02% Ficoll, and 0.02% bovine serum albumin. This mixture was heated in a boiling water bath for 10 min to denature the probe and then plunged into ice, and dithiothreitol was added to a final concentration of 10 mM. Tissue sections were overlaid with sufficient hybridization mixture to cover the entire section (10 to 15 μl) Siliconized glass coverslips were then mounted and sealed with rubber cement. Hybridization was allowed to proceed for 3 days at room temperature. The posthybridization washing was at room temperature and consisted of 2× SSC (1× SSC is 0.15 M sodium chloride plus 0.015 M trisodium citrate, pH 7.0) twice for 5 min each, 2× SSC for 1 h, 2× SSC overnight, 0.2× SSC for 10 min, 0.1× SSC for 10 min, PBS twice for 10 min with a rinse in 0.1% Triton X-100 in between, and dehydration of sections through graded ethanol solutions containing 300 mM ammonium acetate (26). Hybridized slides were dipped in NTB-2 nuclear track emulsion (Kodak, Rochester, N.Y.) diluted with an equal volume of 600 mM ammonium acetate. Exposure was at 4°C for 7 to 10 days, depending on the activity of the probe. The slides were then developed with Kodak D19, stained with hematoxylin and eosin, and mounted with Permount. RNase-treated control slides were digested with a mixture of RNase A (25 μg/ml) and RNase T_1 (40 U/ml) in 2× SSC for 30 min at 37°C immediately after the proteinase K treatment (as described above). Tissue sections were examined on a light microscope by an observer who was blinded to the experimental conditions, and the appearance and location of hybridization signals were recorded. A hybridization signal was defined as a focus of silver grains which was more dense than the background scattering of grains which covered the tissue. Infected and uninfected BGMK cells and muscle harvested on day 7 were used as controls to evaluate the efficiency and specificity of the in situ hybridization technique.

Histologic evaluation of inflammation. The overall level of inflammation in each tissue section was evaluated by light microscopic examination and was performed independently of hybridization signal enumeration. Sections were graded on a scale of 0 to 3 as follows: grade 0, no inflammation; grade 1, some interstitial infiltration by scattered mononuclear cells; grade 2, localized areas of more intense inflammation; grade 3, widespread inflammation with large mononuclear cell infiltrates.

Data analysis. The number of tissue sections varied between the different grades of clinical weakness and inflammation. Thus, to analyze the incidence of persistent virus as it relates to weakness and inflammation, the number of hybridization signals within a given grade was expressed as the hybridization frequency: hybridization frequency = number of hybridization signals/number of tissue sections.

RESULTS

Specificity of in situ hybridization for detection of CVB1. Optimum conditions for in situ hybridization were determined by using proximal hindquarter muscle sections from animals at day 7 postinfection, when virus titers are at their peak (18, 23). During acute infection, CVB1 showed a multifocal distribution in muscle from infected animals. Fascicles within the same muscle also contained different amounts of CVB1 RNA as shown by the hybridization signals (Fig. 1A). This distinct pattern of hybridization signal

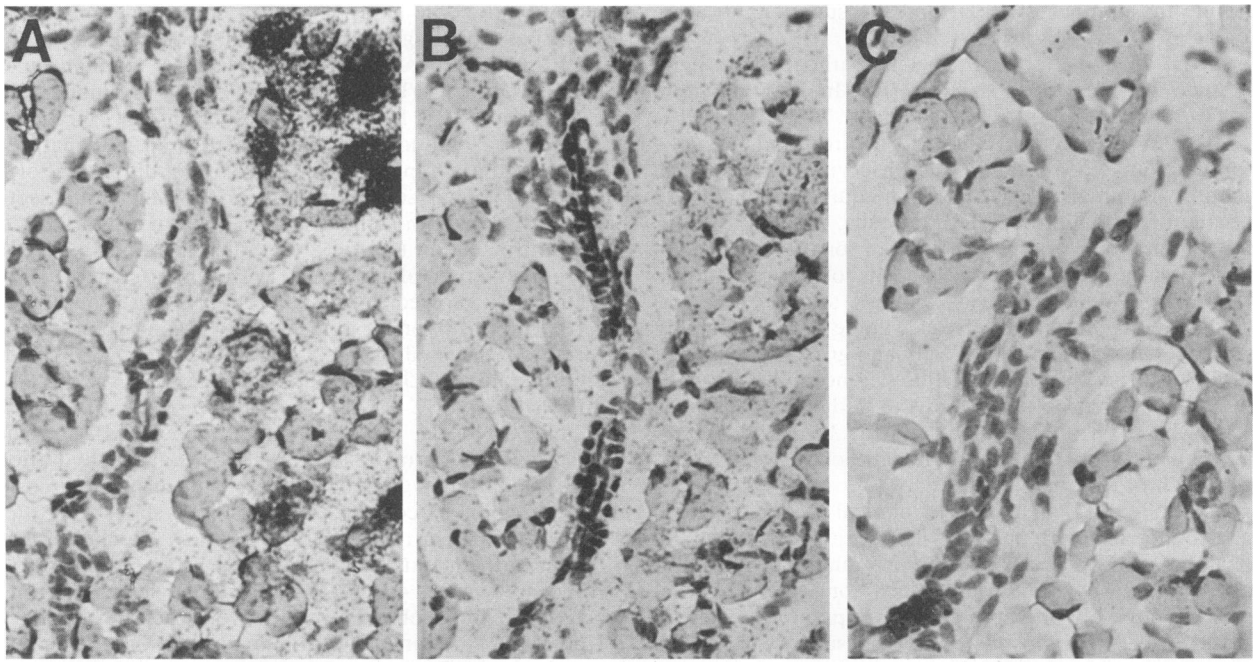

FIG. 1. Specificity of in situ hybridization. Panels A to C are from the same region of three sequential skeletal muscle sections from a CVB1-infected mouse at 7 days postinfection. (A) The enterovirus probe hybridized strongly to hindquarter muscle harvested during the acute infection. CVB1 showed a focal distribution among fascicles within the same muscle. (B) These hybridization signals were greatly reduced by prehybridization treatment with RNase. (C) There was no hybridization of the p2732B plasmid backbone negative control probe. Magnification, ×250.

was reproduced on sequential cross-sections. Longitudinally oriented muscle sections confirmed that virus was generally distributed along individual muscle fibers (results not shown). Prehybridization treatment of infected muscle with RNase abolished the hybridization signal (Fig. 1B), while the negative control probe p2732B did not hybridize (Fig. 1C). Muscle from uninfected animals probed with the enterovirus probe did not show any increase in signal over background levels and thus resembled the negative controls shown in Fig. 1B and C (results not shown). Thus, hybridization of the enterovirus probe was specific for RNA in muscle from CVB1-infected animals. Analogous results were obtained with BGMK cells infected in vitro. Hybridization occurred only between the enterovirus probe and infected BGMK cells and not when the infected cells were pretreated with RNase or probed with p2732B (results not shown). The α-actin positive control probe derived from pAM 91 showed strong generalized hybridization to skeletal muscle RNA (results not shown).

Association of chronic weakness with inflammation. At days 28 to 31, there was a clear relationship between hindquarter muscle weakness and inflammation (Table 1). Low-grade inflammation (grades 1 and 2) occurred in more than half of the tissue sections from infected animals which displayed no visible sign of clinical weakness (grade 0). As the severity of clinical disease increased to grade 2, there was a broader distribution of the degree of inflammation and a substantial increase in the number of sections with grade 2 inflammation. Animals with the greatest amount of clinical disease (grade 3) had almost exclusively grade 2 or 3 inflammation. Similar to the distribution of virus, inflammation was focal and thus there was variability in the amount of inflammation seen in different sections from the same muscle. Inflammation was never observed in the uninfected controls.

Localization of persistent CVB1 in animals with chronic myositis. In situ hybridization was used to screen a total of 169 tissue sections from infected mice and 106 tissue sections from uninfected control mice. Five hamstring sections from infected mice detached from the slide during the hybridization procedure, leaving 82 sections from hamstring muscle and 87 sections from quadriceps muscle. Since the distribution of hybridization signals in the hamstring and quadriceps muscles was similar (a total of 78 signals in the hamstring and 98 signals in the quadriceps), these data were combined. Examination of tissue revealed that there were three distinct histopathology patterns (HPP-1, HPP-2, and HPP-3) based on the pattern of grains, the signal location,

TABLE 1. Clinical hindquarter weakness and inflammation in CVB-1-infected mice[a]

Clinical weakness group	Inflammation[b]				Total no. of hind limbs	Total no. of sections
	0	1	2	3		
Control	100	0	0	0	12	106
0	42	55	3	0	7	40
1	0	100	0	0	2	16
2	31	12	50	7	5	32
3	0	2	58	40	10	81

[a] At 28 to 31 days postinfection, clinical weakness of each hind limb was graded separately on a scale of 0 to 3 as described in Materials and Methods. Tissue sections were cut from hamstring and quadriceps muscles and were graded individually for inflammation on a scale of 0 to 3 as described in Materials and Methods. None of the control animals showed evidence of hindquarter muscle weakness or inflammation.

[b] The inflammation data are expressed as a percentage of the total number of sections examined in each clinical weakness group. The chi-square test comparing the frequency of weakness with inflammation in the infected animals was highly significant with $P < 0.005$.

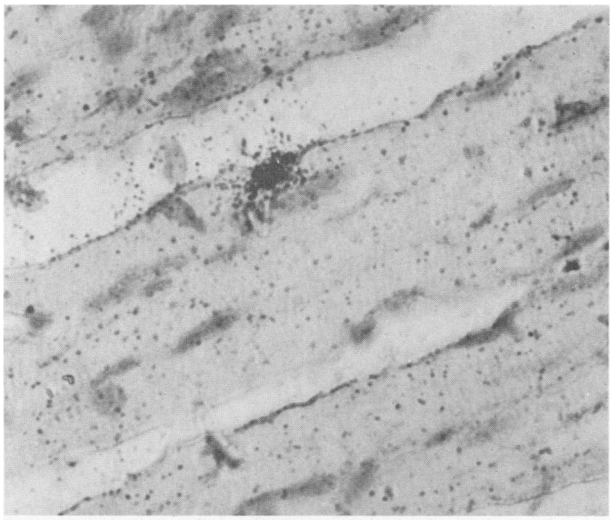

FIG. 2. HPP-1 in quadriceps muscle at 28 days postinfection. A single hybridization signal is pictured. This signal is over the cytoplasm of an intact muscle fiber and is not closely associated with foci of muscle inflammation or necrosis. Magnification, ×400.

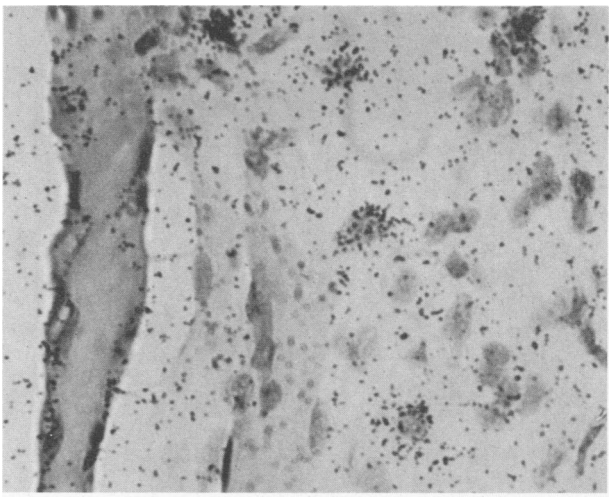

FIG. 4. HPP-3 in hamstring muscle at 31 days postinfection. Hybridization signals can be seen within five infiltrating mononuclear cells in an area of intense tissue destruction bordered by necrotic muscle fibers. Magnification, ×400.

and the accompanying histopathology. In histopathology pattern 1 (HPP-1), virus was identified in muscle fibers which otherwise appeared to be normal and were not closely associated with foci of inflammatory cells (Fig. 2). These signals were sharp, discrete collections of grains. Individual signals were not clustered and were not reproduced on adjacent tissue sections. A total of 57 HPP-1 signals was identified. In HPP-2, virus persisted in necrotic muscle fibers that were surrounded by mononuclear inflammatory cells (Fig. 3). This type of signal showed a less dense pattern of grains than the HPP-1 signal. It was reproduced on adjacent sections, and there appeared to be some clustering of these infected fibers within the muscle. Ninety-two HPP-2 signals were observed. Finally, virus contained within mononuclear cells infiltrating a region where muscle had been extensively destroyed was typical of HPP-3 (Fig. 4). This was a rare occurrence, appearing in the right hamstring of one animal with grade 2 weakness in this leg. However, it was very reproducible since there were many infected mononuclear cells within the boundaries of this damaged region, and sequential sections also contained infected mononuclear cells (a total of 27 signals was counted within three adjacent tissue sections). The general appearance of the HPP-3 signal showed a more intense concentration of grains both at the cell periphery and at one pole of the infected cell, resembling the signal observed in BGMK cells infected in vitro. This particular animal displayed all three HPPs. The right hamstring muscle also had HPP-2, while the muscle of the left leg, which displayed a grade 3 weakness, showed both HPP-1 and HPP-2. Overall, every one of the 12 infected animals contained persistent CVB1. Both HPP-1 and HPP-2 were found in nine mice displaying varying grades of weakness. Two mice with grade 3 weakness in both hind limbs exhibited HPP-2 only, while in one mouse with grade 0 disease only HPP-1 was observed. A few background hybridization signals were observed in three uninfected control animals. These signals were discrete and located directly over myofibers, although they occurred at a very low frequency (five signals out of a total of 106 tissue sections). None of the three HPPs was observed in muscle harvested at day 7. However, the histopathology was quite different during the acute phase, with diffuse inflammation containing polymorphonuclear leukocytes and lymphocytes accompanied by widespread myocyte necrosis. Intense hybridization signals reflected the high level of intracellular replicating virus and sometimes masked the underlying histopathology.

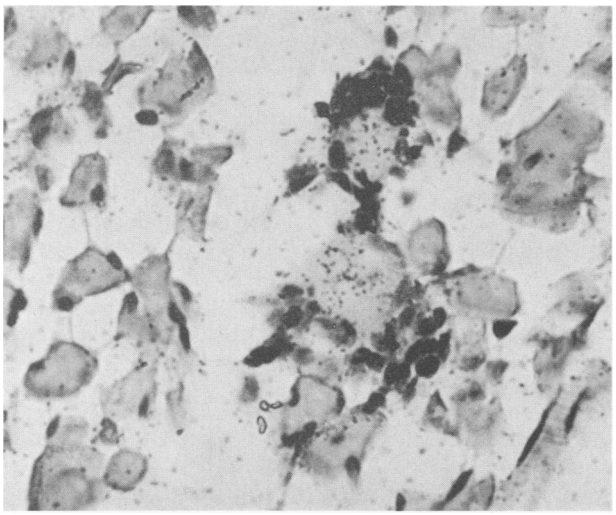

FIG. 3. HPP-2 in quadriceps muscle at 31 days postinfection. Hybridization signal is shown within two adjacent necrotic muscle fibers that are surrounded by inflammatory cells. The signal typically appeared as a less dense collection of grains than that for HPP-1. Magnification, ×400.

Relationship between virus persistence, clinical weakness, and inflammation. A strong positive trend was observed between persistence of CVB1 and the manifestation of clinical weakness (Fig. 5). The frequency of the total number of hybridization signals in animals with grade 2 or 3 weakness was roughly twice that of animals with grade 0 or 1 weakness and at least 24 times greater than the background signal found in uninfected controls. Again, signals in necrotic fibers (HPP-2) and infiltrating mononuclear cells

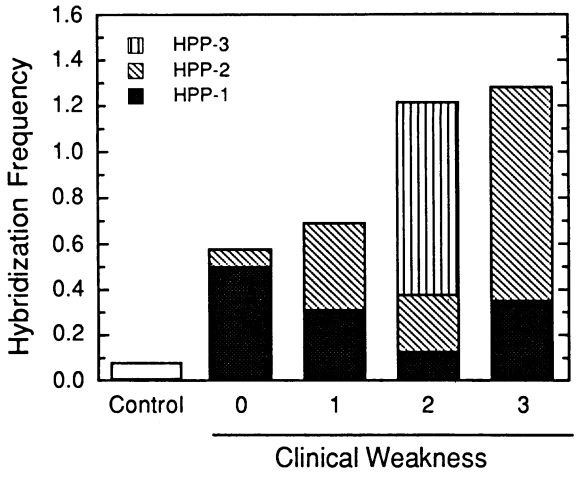

FIG. 5. CVB1 persistence in hindquarter muscle of mice displaying different degrees of clinical weakness (grades 0 to 3 as described in Materials and Methods). The hybridization frequency is the number of hybridization signals divided by the number of tissue sections in a given clinical weakness group. The bars are divided to illustrate the proportion of signals associated with HPP-1, HPP-2, and HPP-3 (additional information on HPPs is located in Results). The correlation between clinical disease and persistence was determined for HPP-1 ($r = -0.52$), HPP-2 ($r = 0.85$), and combined HPP-1, 2, and 3 ($r = 0.95$).

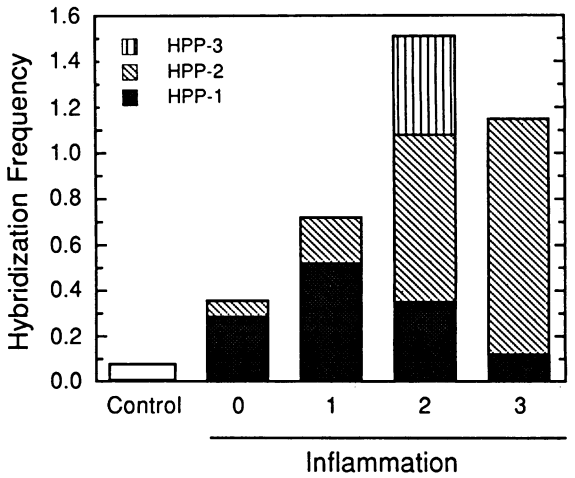

FIG. 6. Relationship between CVB1 persistence and tissue inflammation (grades 0 to 3 as described in Materials and Methods). The hybridization frequency is the number of hybridization signals divided by the number of tissue sections in a given inflammation group. The bars are divided to illustrate the proportion of signals associated with HPP-1, HPP-2, and HPP-3 (additional information on HPPs is located in Results). The correlation between inflammation and persistence was determined for HPP-1 ($r = -0.53$), HPP-2 ($r = 0.98$), and combined HPP-1, 2, and 3 ($r = 0.82$).

(HPP-3) were not evenly distributed throughout the muscle but were more often found as clustered areas of persistent virus containing as many as 18 to 20 signals on a single tissue section. HPP-2 was found at a higher frequency in hind limbs with severe (grade 3) disease, while HPP-1 was slightly more common in infected animals with less disease. The occurrence of HPP-3 was too infrequent to evaluate trends. The distribution of HPP-2 showed an even stronger association with inflammation than with weakness (Fig. 6). Thus, the sections with localized HPP-2 were also more likely to show generalized tissue inflammation. In contrast, there was a negative correlation between the presence of HPP-1 and inflammation. It should be emphasized that tissue sections with HPP-3 were ranked as grade 2 inflammation overall because they did not exhibit the typical large, intensely stained, lymphocytic infiltrates characteristic of grade 3 inflammation. However, persistent virus was directly located in a region of necrosis and inflammation.

DISCUSSION

These data are the first to demonstrate that CVB1 persists in the hindquarter muscle of mice that develop chronic myositis. At 28 to 31 days postinfection, clinical signs of chronic weakness are well developed, and yet this is at least 2 weeks after infectious virus can be detected by plaque assay (23). Viral antigens are also not demonstrable by indirect immunofluorescence after 14 days postinfection (18). This suggests that CVB1 persists at a level which is below the sensitivity of these assays or that persistent CVB1 is an altered, less infectious form of the virus (3, 8). Whatever form this persistent virus may take, its presence correlated strongly with the levels of tissue inflammation and muscle weakness observed in the infected mice. Thus, persistent CVB1 was more frequent in hind limbs with grade 2 or 3 weakness and in tissue sections with grade 2 or 3 inflammation. Infected animals which did not exhibit overt clinical weakness (grade 0) retained lower yet significant levels of persistent virus. However, 58% of the muscle sections from these animals showed histologic evidence of inflammation, indicating that they had subclinical disease. Evaluation of clinical weakness therefore appears to be a less discriminating measure of myositis, and for mice with little or no weakness, inflammation was a better correlate of CVB1 persistence. These data support the hypothesis that CVB1 persistence is involved in the development of chronic myositis. Although we cannot yet exclude the possibility that virus persists as a secondary effect or sequela of muscle damage, other murine models of coxsackievirus-induced disease have shown that viral RNA persists in accordance with defined tissue tropisms. For example, a myocarditic strain of CVB3 persists in myocardium for at least 56 days while a diabetogenic strain of CVB4 has been detected in pancreatic beta cells at 8 weeks postinfection (4, 8).

Three different types of histopathology patterns were associated with persistent virus (HPP-1, HPP-2, and HPP-3). These three HPPs represent potentially different stages in the mechanism of CVB1 persistence. In HPP-1, persistent virus was localized in the cytoplasm of myofibers. Since these myofibers did not look atypical or necrotic, the HPP-1 virus may have a reduced capacity to cause cytopathic effects. Infected myofibers were not visibly under attack by inflammatory cells, and thus in HPP-1 the virus appears to represent a very low grade infection which is undetected by the immune system. In fact, there was a slight inverse correlation between HPP-1 and tissue inflammation. A similar lack of concordance between the presence of virus and inflammation has been observed in other models of enterovirus-induced myopathy (5, 8), and this could represent a stage which is common to some strains of enterovirus. Furthermore, the lack of clustering of HPP-1 suggests that the virus is confined to a very limited space within the myofiber and is probably not undergoing vigorous replication. Taken together, these observations indicate that HPP-1

could represent a defective virus that is less infectious, less lytic, or perhaps interferes with reinfection by the parental virus (3, 13).

In HPP-2, CVB1 persisted within necrotic muscle fibers which were surrounded by inflammatory cells, which fits with the idea that immunologic injury is mediated by a cytotoxic response to virus-infected cells. These signals extended to adjacent cross-sections and in many cases were located near other infected necrotic myofibers. The inflammatory response appeared to be specific for the infected myocytes, since inflammation was not focused on nearby uninfected cells. The diffuse nature of the hybridization signal could be caused by degradation of intracellular viral RNA as the host myofiber is destroyed. A similar virus-related histopathology was recently reported in patients with chronic adult myostis. Muscle biopsy samples from these patients contained foci of inflammation centered around necrotic myofibers containing enterovirus RNA (22).

HPP-3 was located in a region of intense tissue destruction that was infiltrated by nonlymphocytic mononuclear cells. In this particular site, the coxsackievirus probe hybridized only to the infiltrating mononuclear cells. HPP-3 was observed in the right hamstring of a single animal with grade 2 clinical disease in the right leg and grade 3 disease in the left leg. Within this lesion, the distribution of CVB1 was widespread, and there were as many as 18 infected mononuclear cells in a single tissue section. The histopathology of this region was also unique. In the majority of large inflammatory infiltrates observed in other sites the predominant cells were lymphocytic, while the morphology of the cells in this area was more consistent with that of a monocyte-macrophage. Interestingly, persistent enterovirus-infected muscle macrophages in biopsies from some dermatomyositis patients have been detected by using a probe derived from Theiler's murine encephalomyelitis virus (12). Given the focal nature of enterovirus infection and the difficulty in recovering infectious virus from individuals with chronic myositis, infection of these mononuclear cells could be a rare but important event in the mechanism of virus persistence.

The high degree of homology among the coxsackieviruses allows CVB3 cDNA to be used as an enterovirus group-specific probe (7, 20). In our experiments, the specificity of the enterovirus probe for detection of CVB1 was verified by the use of muscle harvested on day 7 when virus titers are at their peak. The enterovirus probe hybridized to muscle from infected animals but not uninfected control animals. Hybridization signal was detected in the cytoplasm of individual fibers and was localized to certain regions of the muscle. A focal distribution of signal was also observed among fascicles within the same muscle. Thus, the distribution of viral RNA mimics the distribution of pathologic changes in muscle, with variations in the distribution, degree, and intensity of the lesions among different fascicles (11, 18, 23). The characteristic HPPs seen at days 28 to 31 were not observed during the acute infection. Necrosis, inflammation, and virus were more widespread at day 7, making such a comparison difficult. Hybridization signals were RNase sensitive, confirming that the enterovirus probe hybridized to an RNA target. Furthermore, the hybridization signals were most likely not caused by artifactual binding of probe DNA since the p2732B plasmid backbone did not yield signal on either infected or uninfected tissue. Specificity of hybridization was confirmed by using uninfected and in vitro-infected BGMK cells.

Our data indicate that CVB1 persistence contributes to the development of murine PM. It remains to be determined whether viral persistence is essential for maintaining the disease once it is established. Initiation could involve an essential role for virus during a critical time period in which clones of myocyte-reactive T cells are established. Once present, these T cells would then be sufficient for long-term maintenance of muscle damage. Alternatively, viral persistence could be critical to chronic disease through continued presentation of virus-derived neoantigens to drive immune system-mediated muscle damage and/or through direct alteration in muscle cell metabolism causing myocyte impairment or death. If infected cells are ultimately destroyed, there must be a mechanism for sustaining viral persistence. Since enteroviruses are not known to integrate into the host genome, this could be accomplished by successive cycles of little or no replication (HPP-1) with intermittent reactivation and infection of regenerated muscle (HPP-2). The virus could also use another kind of cell, such as infiltrating mononuclear cells, to facilitate its dissemination (HPP-3). This animal model of CVB1-induced PM will be useful for understanding mechanisms of enterovirus persistence and the relationship between virus persistence and chronic myositis.

ACKNOWLEDGMENTS

We thank Reinhard Kandolf for the pCB3-M1 clone, Ashley Haase for expert advice on performing in situ hybridization, and Robert Roelofs for assistance in interpretation of muscle histology.

This work was supported by Public Health Service grant AI31101 from the National Institutes of Health (R.P.M.) and grants from the Minnesota Chapter of the Arthritis Foundation (P.E.T.) and the Veterans Administration (S.R.Y.).

REFERENCES

1. **Bocharov, E. V., and O. V. Shalaurova.** 1984. Persistence of coxsackie B1 virus in Balb/c mice. Acta Virol. **28**:345.
2. **Bowles, N. E., V. Dubowitz, C. A. Sewry, and L. C. Archard.** 1987. Dermatomyositis, polymyositis, and coxsackie-B-virus infection. Lancet **i**:1004–1007.
3. **Chatterjee, N. K., and C. Nejman.** 1985. Membrane-bound virions of coxsackievirus B4: cellular localization, analysis of the genomic RNA, genome-linked protein, and effect on host macromolecular synthesis. Arch. Virol. **84**:105–118.
4. **Chatterjee, N. K., and C. Nejman.** 1988. Insulin mRNA content in pancreatic beta cells of coxsackievirus B4-induced diabetic mice. Mol. Cell. Endocrinol. **55**:193–202.
5. **Cronin, M. E., L. A. Love, F. W. Miller, P. R. McClintock, and P. H. Plotz.** 1988. The natural history of encephalomyocarditis virus-induced myositis and myocarditis in mice: viral persistence demonstrated by in situ hybridization. J. Exp. Med. **168**:1639–1648.
6. **Haase, A., M. Brahic, L. Stowring, and H. Blum.** 1984. Detection of viral nucleic acids by in situ hybridization. Methods Virol. **7**:189–226.
7. **Hyypiä, T., P. Stålhandske, R. Vainionpää, and U. Pettersson.** 1984. Detection of enteroviruses by spot hybridization. J. Clin. Microbiol. **19**:436–438.
8. **Kandolf, R., D. Ameis, P. Kirschner, A. Canu, and P. H. Hofschneider.** 1987. In situ detection of enteroviral genomes in myocardial cells by nucleic acid hybridization: an approach to the diagnosis of viral heart disease. Proc. Natl. Acad. Sci. USA **84**:6272–6276.
9. **Kandolf, R., and P. H. Hofschneider.** 1985. Molecular cloning of the genome of a cardiotropic coxsackie B3 virus: full-length reverse-transcribed recombinant cDNA generates infectious virus in mammalian cells. Proc. Natl. Acad. Sci. USA **82**:4818–4822.
10. **Minty, A. J., M. Caravatti, B. Robert, A. Cohen, P. Daubas, A. Weydert, F. Gros, and M. E. Buckingham.** 1981. Mouse actin messenger RNAs: construction and characterization of recombinant plasmid molecule containing a complementary DNA

transcript of mouse α-actin mRNA. J. Biol. Chem. **256**:1008–1014.
11. **Ray, C. G., L. L. Minnich, and P. C. Johnson.** 1979. Selective polymyositis induced by coxsackievirus B1 in mice. J. Infect. Dis. **140**:239–243.
12. **Rosenberg, N. L., H. A. Rotbart, M. J. Abzug, S. P. Ringel, and M. J. Levin.** 1989. Evidence for a novel picornavirus in human dermatomyositis. Ann. Neurol. **26**:204–209.
13. **Rueckert, R. R.** 1985. Picornaviruses and their replication, p. 705–738. *In* B. Fields (ed.), Virology. Raven Press, New York.
14. **Sambrook, J., E. F. Fritsch, and T. Maniatis.** 1989. Molecular cloning: a laboratory manual, 2nd ed. Cold Spring Harbor Laboratory Press, Cold Spring Harbor, N.Y.
15. **Schiraldi, O., and E. Iandolo.** 1978. Polymyositis accompanying coxsackie virus B2 infection. Infection **6**:32–34.
16. **Schnurr, D. P., and N. J. Schmidt.** 1984. Coxsackievirus B3 persistence and myocarditis in NFR nu/nu and +/nu mice. Med. Microbiol. Immunol. **173**:1–7.
17. **Schnurr, D. P., and N. J. Schmidt.** 1988. Persistent infections, p. 181–201. *In* M. Bendinelli and H. Friedman (ed.), Coxsackieviruses: a general update. Plenum Press, New York.
18. **Strongwater, S. L., K. Dorovini-Zis, R. D. Ball, and T. J. Schnitzer.** 1984. A murine model of polymyositis induced by coxsackievirus B1 (Tucson strain). Arthritis Rheum. **27**:433–442.
19. **Tourtellotte, W. W., A. N. Verity, P. Schmid, S. Martinez, and P. Shapshak.** 1987. Covalent binding of formalin fixed paraffin embedded brain tissue sections to glass slides suitable for in situ hybridization. J. Virol. Methods **15**:87–99.
20. **Tracy, S.** 1985. Comparison of genomic homologies in the coxsackievirus B group by use of cDNA:RNA dot-blot hybridization. J. Clin. Microbiol. **21**:371–374.
21. **Travers, R. L., G. R. Hughes, and J. R. Sewall.** 1977. Coxsackie B neutralization titers in polymyositis/dermatomyositis. Lancet **i**:1268.
22. **Yousef, G. E., D. A. Isenberg, and J. F. Mowbray.** 1990. Detection of enterovirus specific RNA sequences in muscle biopsy specimens from patients with adult onset myositis. Ann. Rheum. Dis. **49**:310–315.
23. **Ytterberg, S. R.** 1987. Coxsackievirus B 1 induced murine polymyositis: acute infection with active virus is required for myositis. J. Rheumatol. **14**:12–18.
24. **Ytterberg, S. R., M. L. Mahowald, and R. P. Messner.** 1987. Coxsackievirus B 1-induced polymyositis. Lack of disease expression in nu/nu mice. J. Clin. Invest. **80**:499–506.
25. **Ytterberg, S. R., M. L. Mahowald, and R. P. Messner.** 1988. T cells are required for coxsackievirus B1 induced murine polymyositis. J. Rheumatol. **15**:475–478.
26. **Zhang, H. Y., G. E. Yousef, N. E. Bowles, L. C. Archard, G. F. Mann, and J. F. Mowbray.** 1988. Detection of enterovirus RNA in experimentally infected mice by molecular hybridisation: specificity of subgenomic probes in quantitative slot blot and in situ hybridisation. J. Med. Virol. **26**:375–386.